



Since January 2020 Elsevier has created a COVID-19 resource centre with free information in English and Mandarin on the novel coronavirus COVID-19. The COVID-19 resource centre is hosted on Elsevier Connect, the company's public news and information website.

Elsevier hereby grants permission to make all its COVID-19-related research that is available on the COVID-19 resource centre - including this research content - immediately available in PubMed Central and other publicly funded repositories, such as the WHO COVID database with rights for unrestricted research re-use and analyses in any form or by any means with acknowledgement of the original source. These permissions are granted for free by Elsevier for as long as the COVID-19 resource centre remains active.



Community vulnerability and mobility: What matters most in spatio-temporal modeling of the COVID-19 pandemic?

Rachel Carroll, Ph.D.^{a,*}, Christopher R. Prentice, Ph.D.^b

^a Department of Mathematics and Statistics, University of North Carolina Wilmington, 601 S College Rd., Wilmington, NC, USA

^b Department of Public and International Affairs, University of North Carolina Wilmington, 601 S College Rd., Wilmington, NC, USA

ARTICLE INFO

Keywords:

COVID-19
Composite measures
Spatio-temporal
Vulnerability
Poisson
Human behavior
Mobility

ABSTRACT

Community vulnerability is widely viewed as an important aspect to consider when modeling disease. Although COVID-19 does disproportionately impact vulnerable populations, human behavior as measured by community mobility is equally influential in understanding disease spread. In this research, we seek to understand which of four composite measures perform best in explaining disease spread and mortality, and we explore the extent to which mobility account for variance in the outcomes of interest. We compare two community mobility measures, three composite measures of community vulnerability, and one composite measure that combines vulnerability and human behavior to assess their relative feasibility in modeling the US COVID-19 pandemic. Extensions – via temporally dependent fixed effect coefficients – of the commonly used Bayesian spatio-temporal Poisson disease mapping models are implemented and compared in terms of goodness of fit as well as estimate precision and viability. A comparison of goodness of fit measures nearly unanimously suggests the human behavior-based models are superior. The duration at residence mobility measure indicates two unique and seemingly inverse relationships between mobility and the COVID-19 pandemic: the findings indicate decreased COVID-19 presence with decreased mobility early in the pandemic and increased COVID-19 presence with decreased mobility later in the pandemic. The early indication is likely influenced by a large presence of state-issued stay at home orders and self-quarantine, while the later indication likely emerges as a consequence of holiday gatherings in a country under limited restrictions. This study implements innovative statistical methods and furnishes results that challenge the generally accepted notion that vulnerability and deprivation are key to understanding disparities in health outcomes. We show that human behavior is equally, if not more important to understanding disease spread. We encourage researchers to build upon the work we start here and continue to explore how other behaviors influence the spread of COVID-19.

1. Introduction

The global pandemic engulfing our globe is taxing hospitals and outpatient clinics, dominating headlines, and occupying a pervasive place in everyday life. As such, the coronavirus 2019 (COVID-19) and its effects are appropriately the focus of much scholarly attention. The already prodigious research output is broad and deep with researchers in fields ranging from epidemiology to public administration to economics investigating a range of research questions. Among the studies we surveyed, authors were concerned with the risk factors for contracting and dying of COVID-19 (Fan et al., 2020; Guha et al., 2020), disease prevalence over time and across various regions (Carroll and Prentice, 2021), mitigation strategies for disease control (Lyu and Wehby, 2020),

financial and employment impacts of the pandemic (Moen et al., 2020), social isolation and its effect on mental health (Douglas et al., 2020; Substance Abuse and Mental Health Services Administration, 2020), and community philanthropy and cross-sector collaborative response (Finchum-Mason et al., 2020). A comprehensive review of these disparate bodies of literature is beyond the scope of this manuscript; nonetheless, we note the breadth of these evolving literatures to set the stage for challenging a common methodological practice that persists across them – namely, employing a variety of measures as proxies for socio-demographic characteristics to explain COVID-19's spread (Campbell et al., 2021; Daras et al., 2021).

The Centers for Disease Control, along with many other entities and scholars, boast socio-demographic disparities including race, age,

* Corresponding author.

E-mail address: carrollr@uncw.edu (R. Carroll).

<https://doi.org/10.1016/j.socscimed.2021.114395>

Received 7 June 2021; Received in revised form 12 August 2021; Accepted 9 September 2021

Available online 11 September 2021

0277-9536/© 2021 Elsevier Ltd. All rights reserved.

ethnicity, poverty status, overcrowded housing conditions, population density, and epidemiological factors as driving forces in the COVID-19 pandemic (Division of Viral Diseases, 2021, 2020). Despite the robust literature suggesting that vulnerable populations are key to modeling the COVID-19 pandemic (Carroll and Prentice, 2021; COVIDCareMap, 2020; Onder et al., 2020; Tai et al., 2020), we hypothesize that human behavior as explained by mobility furnishes a superior metric for explaining the spread of COVID-19 over space and time. Our premise is built on several other studies that show the benefits of stay at home orders (Badr et al., 2020; Carroll and Prentice, 2021) as well as the relationship between mobility and COVID-19 presence in the community (Chen et al., 2020; Lee et al., 2021; Nouvellet et al., 2021; Rashed and Hirata, 2021).

COVID-19 caused the first global pandemic wherein technology and research are able to forecast and model the disease in near real-time (Chen et al., 2020; Rashed and Hirata, 2021). Selecting the proper measures for this work is paramount in understanding and mitigating disease spread, and the full array of measures needed to model the spread of COVID-19 are still being identified. Efforts are underway to construct indices that will theoretically help researchers and practitioners identify the factors that increase community vulnerability to the pandemic (Daras et al., 2021; Marvel et al., 2021). In this research, we examine and compare community mobility measured by Google (Google LLC, n.d.) to four composite metrics for capturing vulnerability in a given area, two commonly employed in other literatures and two developed specifically for the COVID-19 pandemic. The mobility measures represent workplace related movement and duration at residence. Alternatively, the vulnerability measures include the Area Deprivation Index (ADI), Social Vulnerability Index (SVI), the COVID-19 Community Vulnerability Index (CCVI), and the COVID-19 Pandemic Vulnerability Index (PVI) (Agency for Toxic Substances and Disease Registry, 2018; Kind et al., 2014; Marvel et al., 2021; Singh, 2003; Surgo Foundarion, 2020).

ADI and SVI – produced before the onset of COVID-19 – are employed extensively in the public health and medical literatures and are important indicators for predicting various chronic and acute health outcomes, medication adherence, and hospital readmission (Agency for Toxic Substances and Disease Registry, 2018; Kind and Buckingham, 2018). We hypothesize that these measures are more limited for modeling of COVID-19 transmission since these do not account for public policy, epidemiological and health system factors, and human behavior which certainly also play a role, as other studies have noted (Chen et al., 2020; Lee et al., 2021; Rashed and Hirata, 2021). Hence, we incorporate two additional composite measures developed specifically to understand vulnerability during the COVID-19 pandemic: CCVI and PVI. Note that one of the factors that comprises PVI is a measure of social distancing to account for human behavior, a feature we suspect is useful for modeling COVID-19. Finally, we supplement the composite measures with a key variable noted in recent COVID-19 literature – mobility – to see whether these patterns have similar or greater associations with the outcomes of interest (Badr et al., 2020; Campbell et al., 2021). We expect, as other scholars have suggested, that modeling human behavior is necessary for understanding COVID-19 disease transmission. In their analysis of mobility patterns in a sample of U.S. counties, Badr et al. found that mobility patterns are strongly correlated with changes in COVID-19 case growth rates (Badr et al., 2020).

In this research, we seek to understand which of the four composite measures perform best in explaining disease spread and mortality, and we explore the extent to which mobility (or the lack thereof) account for variance in the outcomes of interest. First, we detail our data, variable operationalization, and methodological approach. Next, we present results from the spatial and temporal analysis and offer a discussion of the relevant findings. We conclude with implications of our research for scholars, public health practitioners, and policymakers.

2. Materials and methods

2.1. Data

Consistent with Carroll and Prentice, we use the health region as our spatial unit of analysis to reduce zero inflation in and dimension of the data (Carroll and Prentice, 2021; Day et al., 2019). Specifically, data at the U.S. county level results in 7601 (4.8% of weeks/counties) zero counts while data at the U.S. health region level results in 107 (0.6% of weeks/regions) zero counts. Our temporal unit for these data is weeks. While the data is released daily, reducing the temporal unit to weeks reduces the dimension of the model and limits the bias from data reporting errors and delays. The data presented here represent March 23, 2020 to March 7, 2021.

2.1.1. Outcome measures

Outcome data (dependent variables) were sourced from the Johns Hopkins University Center for Systems Science and Engineering (Dong et al., 2020). Data for this study were geographically constrained to the United States. We examined three discrete, count outcomes: number of confirmed cases, number of new cases, and number of deaths. Since there could be differences in covariate relationships based on the region of the country considered, we made an estimation for the US as a whole and apportion the counts into the following regions as defined by the US Census Bureau (Geography Division. U.S. Department of Commerce Economics and Statistics Administration. U.S. Census Bureau, 1984): South (S), West (W), Midwest (MW), and Northeast (NE).

2.1.2. Measures of community mobility

Reports aimed at describing community movement for the benefit of public health officials were made available by Google early in the pandemic and have been maintained since that time (Google LLC, n.d.). Google makes these mobility metrics publicly available and categorizes mobility by type or purpose of movement: grocery and pharmacy, parks, transit stations, retail and recreation, residential, and workplaces. Mobility is calculated as the percent daily change in relation to a baseline median mobility established using January 3, 2020 to February 6, 2020 as the pre-pandemic baseline. Only users who opted into Location History on their Google Account are captured in this measure. Positive values indicate more category-specific mobility compared to the baseline and negative values indicate less category-specific mobility compared to the baseline.

For this study, we considered work- and residential-related mobility as options for our independent variable where work-related mobility is defined as percent change in total visitors to areas defined as places of work while residential-related mobility is defined as percent change in duration at areas defined as residential locations. These daily data are available at the US county level. We aggregated these measures by time and space to represent weekly information for each health region – i.e., median percent change for a given health region each week. Where too few data points are captured, Google assigns those observations as missing to avoid issues pertaining to privacy. Despite our aggregations to weekly information by health region, we still had some missingness: 0.9% for work and 5.7% for residential. We imputed by carrying the last observation forward.

2.1.3. Measures of community vulnerability

Four different composite measures of community vulnerability were considered here as alternatives for the independent variable: Area Deprivation Index (ADI), Social Vulnerability Index (SVI), COVID-19 Community Vulnerability Index (CCVI), and the COVID-19 Pandemic Vulnerability Index (PVI). The ADI, SVI, and CCVI measures are spatial only and remain constant over time, whereas the PVI is dynamic and changes over time.

Developed by Singh and refined over time, ADI uses 17 Census poverty, education, housing and employment indicators to measure a

region's socioeconomic disadvantage and can be used to gain "improved insight into the sociobiological mechanisms that underlie health disparities, which could, in turn, facilitate the development of improved therapeutics and interventions" (Kind and Buckingham, 2018; Singh, 2003). Health systems and healthcare providers can use the ADI to target program delivery by geographic location based on the area of greatest disadvantage. Higher ADI values indicate higher levels of disadvantage in a region (Kind et al., 2014; Singh, 2003).

The next composite metric – SVI – captures social vulnerability, which refers to the resilience of communities when confronted by external stresses on human health, stresses such as natural or human-caused disasters, or disease outbreaks. Reducing social vulnerability can decrease both human suffering and economic loss. The Centers for Disease Control and Prevention's (CDC) Social Vulnerability Index uses 15 U.S. Census variables at the tract level to help local officials identify communities that may need support in preparing for hazards; or recovering from disaster (Agency for Toxic Substances and Disease Registry, 2018). SVI integrates measures representing socioeconomic status, household composition and disability, minority status and language, and housing type and transportation (Agency for Toxic Substances and Disease Registry, 2018). The Geospatial Research, Analysis, and Services Program (GRASP) created and maintains the CDC's Social Vulnerability Index. Higher scores indicate more vulnerability.

The third composite metric – CCVI – is more comprehensive than ADI and SVI, and was developed for modeling vulnerability in the COVID-19 pandemic. Developed by the Surgo Foundation and featured as a CDC resource, CCVI is constructed by adding a range of epidemiological and healthcare system variables to the standard vulnerability measures incorporated in SVI (Surgo Foundation, 2020). CCVI identifies which communities are most vulnerable to coronavirus and least prepared to address it once spread. Mapped to US census tract, county, and state levels, the CCVI can inform COVID-19 planning and mitigation at a granular level. Higher CCVI scores indicate a greater level of vulnerability.

The final composite metric – PVI – is the most comprehensive measure. Developed by researchers in cooperation with the National Institute of Environmental Health Sciences, this index and associated online dashboard was created to give key stakeholders dynamic county-level information that facilitate monitoring disease trajectories, identifying local vulnerability, forecasting key outcomes, and guiding decision making (Marvel et al., 2021). Like CCVI, PVI builds on SVI and adds to that index measures that capture testing rates, social distancing, and disease spread.

2.2. Statistical model

The statistical model applied here is an extension of a model commonly used in disease mapping for aggregated count outcomes, the Bayesian spatio-temporal Poisson Knorr-Held model (Knorr-Held, 2000; Knorr-Held and Besag, 1998; Lawson and Lee, 2017; Lawson, 2013; Lawson et al., 2016; Lesaffre and Lawson, 2013). This model can be defined as follows for health region i and week j :

$$y_{ij} \sim \text{Pois}(\mu_{ij})$$

$$\mu_{ij} = e_{ij}\theta_{ij}$$

$$\text{Spatial only measure} : \log(\theta_{ij}) = x_i\beta_j + u_i + \gamma_j$$

$$\text{Spatio-temporal measure} : \log(\theta_{ij}) = x_{ij}\beta_j + u_i + \gamma_j$$

where y_{ij} is the outcome of interest (count of confirmed cases, new cases, or deaths), μ_{ij} is the mean of the Poisson model, e_{ij} is the expected count, θ_{ij} is the relative risk, x_i or x_{ij} is the mobility or vulnerability measure, β_j is the time varying fixed effect estimate, u_i is the spatial random effect, and γ_j is the temporal random effect. The temporally dependent struc-

ture of β_j offers the extension, a novel aspect to our model in this setting, and allows for fluctuation in the relationship between mobility or vulnerability and the outcome over time. e_{ij} is calculated as the rate of infection across all health regions on a given week times the population at risk for a given health region, which is assumed constant over time. As such, a unique e_{ij} is produced for each health region and week. Given the Bayesian methodology, prior distributions are required for all parameters and they are defined as follows: $\beta_j \sim N(\beta_{j-1}, \tau_{\beta}^{-1})$ for a temporal random walk parameter estimate, $u_i \sim N(0, \tau_u^{-1})$ for an uncorrelated spatial random effect, $\gamma_j \sim N(\gamma_{j-1}, \tau_{\gamma}^{-1})$ for a temporal random walk effect, and all precisions were such that $\tau \sim \text{Gam}(2, 1)$. Finally, inverse logarithms are often used to gain appropriate interpretations of these model parameters since a logarithm link is included in the linear predictor. This transformation allows for estimate interpretations in terms of multiplicative change to the relative risk (θ_{ij}) of the outcome considered. This model description applies to all metrics (mobility and vulnerability), outcomes (confirmed cases, new cases, and deaths), and US Census-defined areas (US, S, W, MW, and NE). [Supplemental Table 1](#) specifically assigns the named model to the appropriate parameterization (x_i or x_{ij}) based on the mobility or vulnerability measure applied.

2.3. Model Comparison Tools

We use the Watanabe-Akaike information criterion (WAIC) to compare these models for goodness of fit (Watanabe, 2010). This measure is a function of the models' deviance estimates and can be written as seen below.

$$\text{WAIC} = \text{DEV}_w + p_w$$

With DEV_w a variation of the deviance $\text{DEV}_w = \sum_i \log(E_{\theta|y}(f(y_i|\theta)))$ and p_w an effective number of parameters calculation such that $p_w = \sum_i V_{\theta|y}(\log(p(y_i|\theta)))$. p_w is considered a penalty term. Smaller values indicate a better fitting model, and a difference of at least 3 units is considered a statistically significant difference in fit. Due to being likelihood based, this measure is only comparable for models with the same outcome. Beyond this goodness of fit measure, we also consider estimate interpretability and feasibility.

2.4. Computational details

R statistical software furnished much of the means for data processing and analysis in the work presented here. Specifically, the R packages `rgdal`, `INLA`, and `fillmap` were necessary for spatial data processing, statistical modeling, and spatial plotting respectively (Bivand et al., 2019; Blangiardo et al., 2013; Carroll, 2016; Carroll et al., 2015; Martins et al., 2013; R Core Team, 2015; Rue et al., 2009; Schrödle and Held, 2011, 2010; Ugarte et al., 2014). Code for the data extraction and manipulation, statistical models, and other applications of this work are available at [this GitHub repository](#).

3. Results

[Fig. 1](#) displays the Google residential median mobility by week for the entire U.S.; images for these measures by Census region are available in the [Supplemental Materials](#). Additional GIFs and images of the mobility and composite measures are available in the [Supplemental Materials](#). The mobility measures suggest more residential and less work mobility than the baseline at the beginning of the pandemic, with a gradual trend towards baseline over time. The South and Northeast health regions appear to return to baseline sooner than the other health regions. The vulnerability measures all show the South region are at higher risk of disease spread and adverse health outcomes. As one would expect, PVI suggests lower vulnerability towards the beginning of the

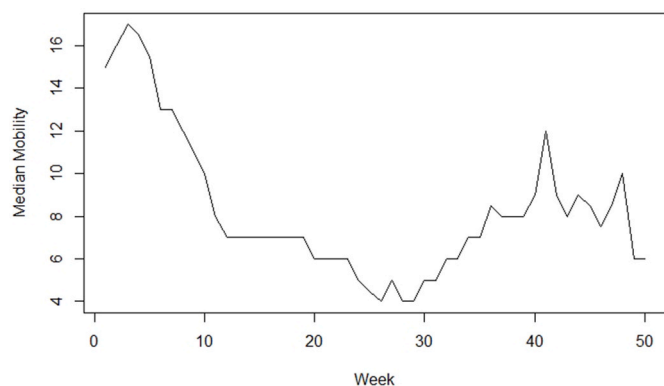


Fig. 1. Median Google residential mobility over time for the entire United States.

pandemic and generally rises over time. However, parts of the Midwest, Northeast, and Alaska remain low, while the West region shows the greatest range in outcomes.

Table 1 displays the goodness of fit measures for the six models, three outcomes, and five areas considered. Details of these measures were described in the Model Comparison Tools section. Consistent with accepted practice, goodness of fit statistics smaller by at least 3 units represent a statistically significant improvement in model fit. In reading the table, it is important to note that only measures within outcomes are comparable; thus, only row-wise comparisons are appropriate. The table shows that PVI and the mobility measures are the best or second best fitting for all models with PVI as the clear winner for 8 of the 15 models (3 outcomes x 5 areas covered). The following is a list of the models that are either the best or second best fitting, presented in descending order from highest to lowest (with counts provided in parentheses): PVI (n = 9), residential mobility (n = 8), work mobility (n = 6), ADI (n = 4), and

SVI (n = 3). Surprisingly, CCVI – a metric specifically developed for describing community vulnerability related to COVID-19 – does not lead to the best fit in any setting, even among the other vulnerability measures.

Whereas the PVI model offered the best fit for the greatest number of outcomes and regions, the estimates showed little consistency across models and seemingly random sharp peaks suggesting increased risk over the study time. The residential mobility model offered more interpretable results and are thus presented below. Fig. 2 displays the time varying parameter estimates associated with the residential mobility metric for the U.S. models (measures across all 15 models are available in the Supplemental Materials). An inverse logarithm was applied to these parameter estimates to offer an interpretation directly related to the multiplicative change in relative risk (θ_{ij}) of the outcome considered. Consequently, an estimate with a 95% credible interval fully less than one (represented by the solid horizontal line) suggests decreased risk while an estimate with an interval fully greater than one suggests increased risk for the given week of the study period. These images include credible interval bounds and the narrow nature of these bounds suggests that our estimates are quite precise over all the models. Most early estimates, particularly between the dash lines that indicate when much of the country was shut down (weeks 2–7 or March 30, 2020 to May 18, 2020), are less than one. This result is interpreted as more residential presence, less COVID-19 and supports the hypothesized benefits of the stay at home orders as a means for reducing disease spread.

Alternatively, many of the estimates between the dotted lines, indicators of the holiday season (weeks 40–42 or December 21, 2020 to January 4, 2021), are greater than one. The interpretation here is more residential presence, more COVID-19, suggesting family gatherings may contribute to disease spread. Finally, most of the estimates for the Northeast are less than one suggesting more residential presence, less COVID-19 throughout most of the pandemic. Estimates for the other measures and models can be interpreted similarly and are included in

Table 1

Goodness of fit measures for the six models across, three outcomes, and five areas considered. The darker grey shading indicates the best fitting model and the lighter grey shading indicates the second best fitting model.

Area Covered/ Outcome	CCVI model	SVI model	ADI model	Work model	Residential model	PVI model
United States						
Confirmed	24246318	24129536	23978034	24141699	24127468	23245846
New	6534349	6527923	6533715	6524345	6514141	6405328
Deaths	2945570	2921433	2902723	2893606	2883996	2729174
South						
Confirmed	5206477	5095613	5128055	5073996	5094847	5082015
New	1585768	1585446	1586026	1585944	1587769	1573245
Deaths	490761	474663	475197	466869	476772	475566
West						
Confirmed	3696408	3694770	3682763	3395637	3383675	3551055
New	1114756	1114443	1105220	1093984	1101149	1086681
Deaths	224482	222977	222450	215982	216833	219625
Midwest						
Confirmed	2815972	2702110	2773928	2710363	2785598	2684561
New	804960	792815	796682	786771	786319	782517
Deaths	297619	280434	295935	269222	279668	253563
Northeast						
Confirmed	1919086	1935020	1725252	1860314	1822091	1887330
New	422603	429573	389508	410940	394834	421585
Deaths	247824	252341	228536	240818	239663	245427

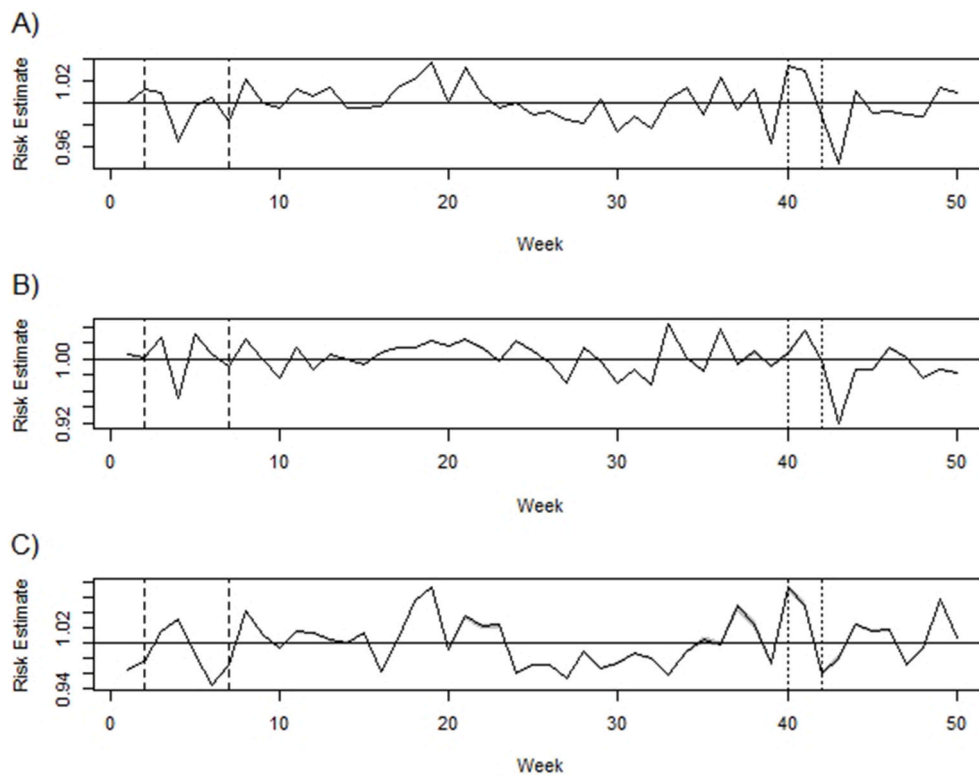


Fig. 2. Time varying parameter estimate from the model using the U.S. Google residential mobility measures for A) confirmed cases, B) new cases, and C) deaths. The solid line displays where the critical value of 1 is on the vertical axis, the dashed lines indicate the time window when much of the country was shut down (weeks 2–7 or March 30, 2020 to May 18, 2020), and the dotted lines indicates the holiday season (weeks 40–42 or December 21, 2020 to January 4, 2021).

the supplemental materials.

4. Discussion

This manuscript examines an array of options for representing mobility, community vulnerability, and the combination of those factors for modeling the COVID-19 pandemic. A comparison of these metrics suggests that mobility measures supersede community vulnerability measures in this setting. Varying patterns emerge: whereas some of the observed patterns suggest less mobility with less COVID-19 presence early in the pandemic, others indicate less mobility with more COVID-19 presence, particularly around the holiday season. As one might expect, we did not see clear trends in the vulnerability measures. Underlying vulnerability is not typically subject to rapid change and hence would not fluctuate as much as mobility. PVI combines vulnerability and mobility information and thus achieves the best fit for modeling of the pandemic. However, estimates associated with the mobility measures appear more informative, which could indicate overfitting in the PVI model.

The mobility models offer two interesting findings: 1) reduced COVID-19 with increased residential presence early in the pandemic, and 2) increased COVID-19 with increased residential presence later in the pandemic, particularly around the holiday season. Whereas these relationships appear contradictory on the surface, we contend they vary because of the type of residential presence during these different times. The first observation likely reflects the effects of stay at home orders and supports the idea of using social distancing to reduce the incidence of COVID-19 (Carroll and Prentice, 2021). The second observation demonstrates an inverse relationship between residential presence and COVID-19 incidence, and notably occurs during the holiday season. The timing suggests families may be gathering in residences, which increases the likelihood of transmission and justifies the importance of social distancing for limiting the spread of COVID-19.

In addition to the models presented in this paper, we also explored models without time-varying coefficients as well as an alternative mobility measure. The goodness of fit measures for the models without time-varying coefficients were higher suggesting worse fit without this added flexibility. This finding underscores the necessity for allowing for a fluctuating relationship between our metrics, particularly the mobility metrics, and COVID-19. We also explored an alternative metric of mobility, specifically the mobility metric produced by Descartes Labs (Warren and Skillman, 2020). This measure showed some similarity in trends over time to the Google work mobility measure. However, there was evidence missing were not random, and indeed no data were available for the entire study period in certain health regions. Therefore, Google mobility data were deemed superior for use in this analysis.

The results presented here are not without limitations. We operate under the assumption that the available data is mostly without error, which may or may not be the case. The model is robust to misspecification, but does not account for this possible error. Additionally, the mobility measures may include missing and potentially not representative data due to privacy issues. Individuals need to opt into Location History on their Google Account to captured in these data. Finally, the statistical model offers a high degree of flexibility through the temporally dependent coefficient estimates, but we make the assumption that the coefficient estimates apply across all health regions in the model for a given week.

These findings have numerous implications for research, including most notably that latently observed community vulnerability is not as important for understanding differences in COVID-19 transmission and health outcomes as human behavior. Future research should follow the lessons learned here and incorporate variables that capture both vulnerability and behavior, as well as potentially other mitigating factors. For example, modeling the next phase of the pandemic will likely require incorporating vaccination information in addition to the measures explored here in order to understand disease spread. Perhaps PVI

can be updated or amended to include vaccine information, building on the measure's current inclusion of infection rates (Marvel et al., 2021). We suspect that as more individuals are inoculated, mobility and social distancing will play a less important role. However, this assumption does not account for the relative risks imposed by COVID-19 variants or nonvaccinated individuals.

5. Conclusion

This manuscript offers an important first step in understanding how human behavior and community vulnerability relate to COVID-19. The relationships uncovered here suggest notable results with respect to social distancing and community presence of COVID-19 and serve as a basis upon which future research can expand. Community vulnerability is widely viewed as an important aspect to consider when modeling disparities in health outcomes including COVID-19. Although COVID-19 does disproportionately impact vulnerable populations, human behavior as measured by community mobility is equally influential in understanding disease spread. Indeed, we show that measures of vulnerability that include mobility are most effective for modeling COVID-19. We encourage researchers to build upon these findings by modeling various additional measures of human behavior that may improve our understanding of how these factors affect the spread of COVID-19 and resulting health disparities.

Credit Author Statement

Rachel Carroll: Data curation, Formal analysis, Methodology, Software, Visualization, Writing – original draft, Writing – review & editing. Christopher R. Prentice: Data curation, Writing – original draft, Writing – review & editing.

Acknowledgements

This research was supported in part by the University of North Carolina's Center for Social Impact with special thanks to Cape Fear Collective.

Appendix A. Supplementary data

Supplementary data to this article can be found online at <https://doi.org/10.1016/j.socscimed.2021.114395>.

References

- Agency for Toxic Substances and Disease Registry, 2018. Social Vulnerability Index (SVI).
- Badr, H.S., Du, H., Marshall, M., Dong, E., Squire, M.M., Gardner, L.M., 2020. Association between mobility patterns and COVID-19 transmission in the USA: a mathematical modelling study. *Lancet Infect. Dis.* 20, 1247–1254. [https://doi.org/10.1016/S1473-3099\(20\)30553-3](https://doi.org/10.1016/S1473-3099(20)30553-3).
- Bivand, R., Rowlingson, B., Tim, K., 2019. Rgdal: Bindings for the "Geospatial" Data.
- Blangiardo, M., Cameletti, M., Baio, G., Rue, H., 2013. Spatial and spatio-temporal models with R-INLA. *Spat Spat. Epidemiology* 4, 33–49. <https://doi.org/10.1016/j.sste.2012.12.001>.
- Campbell, M., Marek, L., Wiki, J., Hobbs, M., Sabel, C.E., McCarthy, J., Kingham, S., 2021. National movement patterns during the COVID-19 pandemic in New Zealand: the unexplored role of neighbourhood deprivation. *J. Epidemiol. Community Health* jech-2020-216108 75 (9), 903–905. <https://doi.org/10.1136/jech-2020-216108>.
- Carroll, R., 2016. Fillmap: Create Maps with SpatialPolygons Objects.
- Carroll, R., Prentice, C., 2021. Using Spatial and Temporal Modeling to Visualize the Effects of U.S. State Issued Stay at Home Orders on COVID-19 (submitted for publication).
- Carroll, R., Lawson, A.B., Faes, C., Kirby, R.S., Aregay, M., Watjou, K., 2015. Comparing INLA and OpenBUGS for hierarchical Poisson modeling in disease mapping. *Spat Spat. Epidemiol* 14 (15), 45–54. <https://doi.org/10.1016/j.sste.2015.08.001>.
- Chen, H., He, J., Song, W., Wang, L., Wang, J., Chen, Y., 2020. Modeling and interpreting the COVID-19 intervention strategy of China: a human mobility view. *PLoS One* 15, e0242761. <https://doi.org/10.1371/journal.pone.0242761>.
- COVIDCareMap, 2020. Mapping US health system capacity needs to care for COVID-19 patients.
- Daras, K., Alexiou, A., Rose, T.C., Buchan, I., Taylor-Robinson, D., Barr, B., 2021. How does vulnerability to COVID-19 vary between communities in England? Developing a small area vulnerability index (SAVI). *J. Epidemiol.* <https://doi.org/10.1136/jech-2020-215227>. *Community Health* jech-2020-215227.
- Day, K., Carroll, R., Zhao, S., 2019. A comparison of spatial resolution in North Carolina. *High Sch. J. Mat.* (in press).
- Division of Viral Diseases, 2020. COVID-19 racial and ethnic health disparities [WWW Document]. Natl. Cent. Immun. Respir. Dis. Centers Dis. Control. URL <https://www.cdc.gov/coronavirus/2019-ncov/community/health-equity/racial-ethnic-disparities/increased-risk-exposure.html>, 3.29.21.
- Division of Viral Diseases, 2021. Rural communities [WWW document]. Natl. Cent. Immun. Respir. Dis. Centers Dis. Control. URL <https://www.cdc.gov/coronavirus/2019-ncov/need-extra-precautions/other-at-risk-populations/rural-communities.html>, 3.29.21.
- Dong, E., Du, H., Gardner, L., 2020. An interactive web-based dashboard to track COVID-19 in real time. *Lancet Infect. Dis.* 20, 533–534. [https://doi.org/10.1016/S1473-3099\(20\)30120-1](https://doi.org/10.1016/S1473-3099(20)30120-1).
- Douglas, M., Katikireddi, S.V., Taulbut, M., McKee, M., McCartney, G., 2020. Mitigating the wider health effects of covid-19 pandemic response. *BMJ.* <https://doi.org/10.1136/bmj.m1557>.
- Fan, V.S., Dominitz, J.A., Eastment, M.C., Locke, E., Green, P., Berry, K., O'Hare, A.M., Shah, J.A., Crothers, K., Ioannou, G.N., 2020. Risk Factors for testing positive for SARS-CoV-2 in a national US healthcare system. *Clin. Infect. Dis.* <https://doi.org/10.1093/cid/ciaa1624>.
- Fincham-Mason, E., Husted, K., Suárez, D., 2020. Philanthropic foundation responses to COVID-19. *Nonprofit Voluntary Sect. Q.* 49, 1129–1141. <https://doi.org/10.1177/0899764020966047>.
- Foundarion, Surgo, 2020. The COVID-19 Community Vulnerability Index (CCVI). Geography Division. U.S. Department of Commerce Economics and Statistics Administration. U.S. Census Bureau, 1984. Census regions and divisions of the United States [WWW Document]. URL https://www2.census.gov/geo/pdfs/maps-data/maps/reference/us_regdiv.pdf.
- Google, L.L.C., Google, n.d.. COVID-19 community mobility reports [WWW document]. URL <https://www.google.com/covid19/mobility/>, 3.16.21.
- Guha, A., Bonsu, J.M., Dey, A.K., Addison, D., 2020. Community and Socioeconomic Factors Associated with COVID-19 in the United States: zip code level cross sectional analysis. medRxiv. <https://doi.org/10.1101/2020.04.19.20071944> in press.
- Kind, A.J.H., Buckingham, W.R., 2018. Making neighborhood-disadvantage metrics accessible — the neighborhood atlas. *N. Engl. J. Med.* 378, 2456–2458. <https://doi.org/10.1056/NEJMp1802313>.
- Kind, A.J.H., Jencks, S., Brock, J., Yu, M., Bartels, C., Ehlenbach, W., Greenberg, C., Smith, M., 2014. Neighborhood socioeconomic disadvantage and 30-day rehospitalization. *Ann. Intern. Med.* 161, 765. <https://doi.org/10.7326/M13-2946>.
- Knorr-Held, L., 2000. Bayesian modeling of inseparable space-time variation in disease risk. *Stat. Med.* 19, 2555–2567.
- Knorr-Held, L., Besag, J., 1998. Modelling risk from a disease in time and space. *Stat. Med.* 17, 2045–2060. [https://doi.org/10.1002/\(sici\)1097-0258\(19980930\)17:18<2045::aid-sim943>3.0.co;2-p](https://doi.org/10.1002/(sici)1097-0258(19980930)17:18<2045::aid-sim943>3.0.co;2-p).
- Lawson, A.B., 2013. Bayesian Disease Mapping: Hierarchical Modeling in Spatial Epidemiology, second ed. CRC Press, Boca Raton, FL.
- Lawson, A., Lee, D., 2017. Bayesian Disease Mapping for Public Health, pp. 443–481. <https://doi.org/10.1016/bs.host.2017.05.001>.
- Lawson, A.B., Banerjee, S., Haining, R., Ugarte, M.D., 2016. Handbook of Spatial Epidemiology. CRC Press, Boca Raton, FL.
- Lee, W. Do, Qian, M., Schwanen, T., 2021. The association between socioeconomic status and mobility reductions in the early stage of England's COVID-19 epidemic. *Health Place* 69, 102563. <https://doi.org/10.1016/j.healthplace.2021.102563>.
- Lesaffre, E., Lawson, A.B., 2013. Bayesian Biostatistics, first ed. Wiley, West Sussex, U.K. <https://doi.org/10.1002/978-1-119-94241-2>.
- Lyu, W., Wehby, G.L., 2020. Community use of face masks and COVID-19: evidence from a natural experiment of state mandates in the US. *Health Aff.* 39, 1419–1425. <https://doi.org/10.1377/hlthaff.2020.00818>.
- Martins, T.G., Simpson, D., Lindgren, F., Rue, H., 2013. Bayesian computing with INLA: new features. *Comput. Stat. Data Anal.* 67, 68–83. <https://doi.org/10.1016/j.csda.2013.04.014>.
- Marvel, S.W., House, J.S., Wheeler, M., Song, K., Zhou, Y.-H., Wright, F.A., Chiu, W.A., Rusyn, I., Motsinger-Reif, A., Reif, D.M., 2021. The COVID-19 pandemic vulnerability index (PVI) dashboard: monitoring county-level vulnerability using visualization, statistical modeling, and machine learning. *Environ. Health Perspect.* 129, 017701 <https://doi.org/10.1289/EHP8690>.
- Moen, P., Peditke, J.H., Flood, S., 2020. Disparate disruptions: intersectional COVID-19 employment effects by age, gender, education, and race/ethnicity. *Work. Aging Retire.* 6, 207–228. <https://doi.org/10.1093/workar/waaa013>.
- Nouvellet, P., Bhatia, S., Cori, A., Ainslie, K.E.C., Baguein, M., Bhatt, S., Boonyasiri, A., Brazeau, N.F., Cattarino, L., Cooper, L.V., Coupland, H., Cucunuba, Z.M., Cuomo-Dannenburg, G., Dighe, A., Djafaara, B.A., Dorigatti, I., Eales, O.D., van Elsland, S.L., Nascimento, F.F., FitzJohn, R.G., Gaythorpe, K.A.M., Geidelberg, L., Green, W.D., Hamlet, A., Hauck, K., Hinsley, W., Imai, N., Jeffrey, B., Knock, E., Laydon, D.J., Lees, J.A., Mangal, T., Mellan, T.A., Nedjati-Gilani, G., Parag, K.V., Pons-Salort, M., Ragonnet-Cronin, M., Riley, S., Unwin, H.J.T., Verity, R., Vollmer, M.A.C., Volz, E., Walker, P.G.T., Walters, C.E., Wang, H., Watson, O.J., Whittaker, C., Whittles, L.K., Xi, X., Ferguson, N.M., Donnelly, C.A., 2021. Reduction in mobility and COVID-19 transmission. *Nat. Commun.* 12, 1090. <https://doi.org/10.1038/s41467-021-21358-2>.

- Onder, G., Rezza, G., Brusaferro, S., 2020. Case-fatality rate and characteristics of patients dying in relation to COVID-19 in Italy. *J. Am. Med. Assoc.* <https://doi.org/10.1001/jama.2020.4683>.
- R Core Team, 2015. R: a language and environment for statistical computing. *R Found. Stat. Comput.*
- Rashed, E.A., Hirata, A., 2021. One-year lesson: machine learning prediction of COVID-19 positive cases with meteorological data and mobility estimate in Japan. *Int. J. Environ. Res. Publ. Health* 18, 5736. <https://doi.org/10.3390/ijerph18115736>.
- Rue, H., Martino, S., Chopin, N., 2009. Approximate Bayesian inference for latent Gaussian models using integrated nested Laplace approximations (with discussion). *J. Roy. Stat. Soc. B* 71, 319–392.
- Schrödle, B., Held, L., 2010. A primer on disease mapping and ecological regression using INLA. *Comput. Stat.* 26, 241–258. <https://doi.org/10.1007/s00180-010-0208-2>.
- Schrödle, B., Held, L., 2011. Spatio-temporal disease mapping using INLA. *Environmetrics* 22, 725–734. <https://doi.org/10.1002/env.1065>.
- Singh, G.K., 2003. Area deprivation and widening inequalities in US mortality, 1969–1998. *Am. J. Publ. Health* 93, 1137–1143. <https://doi.org/10.2105/AJPH.93.7.1137>.
- Substance Abuse and Mental Health Services Administration, 2020. Double jeopardy: COVID-19 and behavioral health disparities for black and latino communities in the U.S [WWW Document]. URL <https://www.samhsa.gov/sites/default/files/covid19-behavioral-health-disparities-black-latino-communities.pdf>.
- Tai, D.B.G., Shah, A., Doubeni, C.A., Sia, I.G., Wieland, M.L., 2020. The disproportionate impact of COVID-19 on racial and ethnic minorities in the United States. *Clin. Infect. Dis.* <https://doi.org/10.1093/cid/ciaa815>.
- Ugarte, M.D., Adin, A., Goicoa, T., Militino, A.F., 2014. On fitting spatio-temporal disease mapping models using approximate Bayesian inference. *Stat. Methods Med. Res.* 23, 507–530. <https://doi.org/10.1177/0962280214527528>.
- Warren, M.S., Skillman, S.W., 2020. Mobility changes in response to COVID-19, [WWW document]. Descartes Labs. URL <https://www.descarteslabs.com/mobility/>.
- Watanabe, S., 2010. Asymptotic equivalence of Bayes cross validation and widely applicable information criterion in singular learning theory. *J. Mach. Learn. Res.* 11, 3571–3594, 10.1.1.407.7976.